International Journal of Research
Available at https://edupediapublications.org/journals
e-ISSN: 2348-6848
p-ISSN: 2348-795X
Volume 04 Issue14
November 2017

Maximum Power Point Tracking Of Pv Arrays And Wind Energy System Under Psc With Ic Technique

A.Manjula
Assistant professor
manjualeee@CVSR.ac.in
Anurag Group Of Institutions, Cvsr College Of Engineering

ABSTRACT- *An improved analysis of maximum power point tracking with incremental conductance of wind energy system array under partial shaded condition is proposed in this paper. In this paper we use the IC techinque, it is used to track the maximum power point of the PV source. MPPT can minimize the system cost and maximize the array efficiency. The proposed system is simple and cost effective. In this paper, a novel two-stage MPPT method is presented to overcome this drawback. In the first stage, a method is proposed to determine the occurrence of PSC, and in the second stage, using a new algorithm that is based on ramp change of the duty cycle and continuous sampling from the P-V characteristic of the array, global maximum power point of array is reached. Open loop operation of the proposed method makes its implementation cheap and simple. The IC algorithm was designed to control the duty cycle of Buck Boost converter and to ensure the MPPT work at its maximum efficiency. The method is robust in the face of changing environmental conditions and array characteristics, and has minimum negative impact on the connected power system. By using the simulation results we can analyze the proposed method.*
Index Terms— DC/DC converter, maximum power point tracking (MPPT), Incremental conductance method, Partial shading condition, wind generation system.

INTRODUCTION

Wind power is another most competitive renewable technologies and, in developed countries with good wind resources, onshore wind is often competitive with fossil fuelfired generation. The purpose of this paper is to study and compare three maximum power point tracking (MPPT) methods in a photovoltaic simulation system using IC method.

Numerous maximum power point tracking (MPPT) techniques have been presented and implemented. Some of the conventional and most popular ones are perturb and observe (P&O), incremental conductance (IC), and short circuit current and open circuit voltage. Wind power generation has experienced a tremendous growth in the past decade, and has been recognized as an environmental friendly and economically competitive means of electric power generation. The wind energy system generates power in the form of AC with different voltage and frequency levels in case of variable speed operation. Conventional MPPT techniques are unable to identify the global maximum power point (GMPP) in PSC, and usually track local peaks. Therefore, developing new MPPT techniques for dealing with PSC is necessary.

Generally, a good MPPT algorithm that is also successful in PSC should have the following properties:

1) Tracking the MPP rapidly for getting high efficiency,

2) Simple implementation with a low computational load,

3) Requiring less and cheaper sensors (removing current sensors of boost converter reduces the cost dramatically),

4) Imposing minimum disturbance to the connected grid.

In this paper, a novel MPPT algorithm is presented which is based on ramp change of the duty cycle and continuous sampling from the P-V characteristic of the array. Simple and cheap implementation due to its open loop operation, high and adjustable speed, robust and guaranteed performance in all conditions, and imposing minimum disturbance to the connected power system are advantages of the proposed method. Also, a new algorithm for detecting PSC occurrence on PV array is presented that has performance superiority over present methods.

Wind energy is a clean fuel source. Wind energy doesn't pollute the air like power plants that rely on combustion of fossil fuels, such as coal or natural gas. Wind turbines don't produce atmospheric emissions that increase health problems like asthma or create acid rain or greenhouse gases. Most of these techniques consist of two steps to attain GMPP. In the first step, the neighborhood of GMPP is determined. In [4], after PSC detection, by moving on the load line that is based on short circuit current and open circuit voltage of the array, the operating point moves to the vicinity of the GMPP, and in the second step, the operating point converges to it. One can easily show that this technique is unable to track the GMPP in all PSCs [5].

In these methods, GMPP is obtained by sampling different points of the array P-V characteristic. These methods are mostly successful, but their sampling number is high. Since the GMPP can occur in a wide range of the P-V characteristic, initial sampling must cover the entire curve. This method proposes two methods: the first approach samples the P-V curve and limits the search area based on short circuit current of the modules and the highest local power.

MODELLING OF WIND SYSTEM:

The wind turbine depending on the flow of air in the rotor consists of two or three blades mechanically coupled to an

International Journal of Research
Available at https://edupediapublications.org/journals
e-ISSN: 2348-6848
p-ISSN: 2348-795X
Volume 04 Issue14
November 2017

electric generator. The power captured by the wind turbine is given by relation

$$P_\omega = \frac{1}{2} C_P \rho . A . V_\omega^3 \quad (1)$$

P is the air density, which is equal to 1.225 kglm3, Cp is the power coefficient, Vw is the wind speed in (m/s) and A is the area swept by the rotor inC m2). The amount of aerodynamic torque Tw in (N-m) is given by the ratio between Ihe power extracted from the wind Pw and turbine rotor speed Ww in (rad Is) as follows

$$T_w = P_{\omega w_\omega} \quad (2)$$

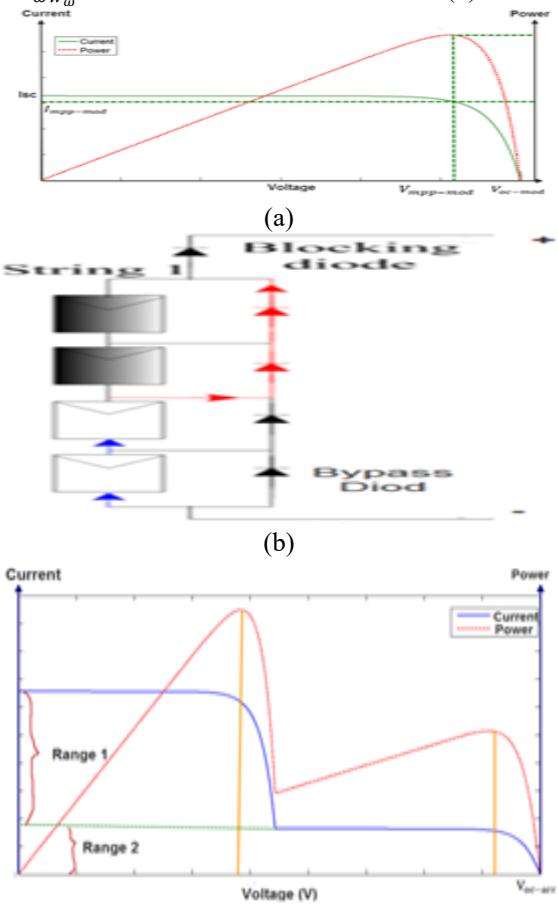

Fig. 1. (a) P-V and I-V characteristics of a typical PV module. (b) Structure of a sample shaded string. (c) P-V and I-V characteristics of the shaded string

The module current is maximum at and is known as short circuit current . For voltages above there will be negative current, but a blocking diode will force it to zero. In 0 (a), I-V and P-V characteristics of a typical solar module under UIC are presented. In UIC, the maximum power point of module and array are unique and are achieved at and , respectively; is a coefficient that is dependent on model parameters of solar module.

Partially Shaded Condition

For simplicity, it is initially supposed that the array under PSC is subjected to two different irradiance levels. The insolated modules of a string drive the string current. Therefore, portion of the string current that is greater than the generated current of shaded modules passes through parallel resistance of the shaded modules and generates negative voltage across them. Thus, the shaded modules consume power instead of generating it. In this condition, not only the overall efficiency drops, but also the shaded modules may be damaged due to hot spots. To prevent this condition, a bypass diode is connected in parallel to each module, to let the extra current of the string pass through it.

Critical Observations under Partially Shading Condition

As explained in the previous subsection, for currents higher than of shaded modules (Range 1), their bypass diodes conduct extra current and cause the voltage across them to be about to . In this situation, the string voltage is equally divided only between the insolated modules. For currents lower than of the shaded modules (Range 2), insolated modules operate in approximately constant voltage area, and therefore, the voltage across each of these modules will be more than and close to . The P-V characteristic of the string has two MPPs. The first one is at and the second MPP occurs when the voltage of one shaded module is about . The string voltage in this local MPP ( ) is bound as follows:

$$N_S V_{mpp-mod} < V_{mpp-2} < n_{sh} V_{mpp-mod} + n_{in} V_{oc-mod}$$

When the irradiance ratio decreases, gets close to the lower bound of (3), and as it increases, moves toward the upper limit. Also, when is too high the upper limit of (3) approaches the lower limit, and gets close to it.

IV OPEN LOOP CONTROL OF BOOST CONVERTER IN PV SYSTEM

In Fig. 2, a two-stage grid connected solar system is shown. In the first stage, DC/DC boost converter plays the main role in absorbing power from the PV array by controlling its voltage. In the second stage, an inverter controls the output voltage of the DC/DC converter and generates AC voltage to connect the solar system to the grid. Because of the DC link capacitor between the boost converter and the inverter, there is little coupling between the two stages and the stages can be studied separately [25].

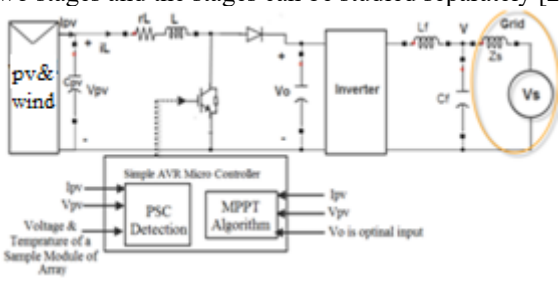

Fig. 3. Overview of a two-stage grid connected PV system structure.

International Journal of Research
Available at https://edupediapublications.org/journals
e-ISSN: 2348-6848
p-ISSN: 2348-795X
Volume 04 Issue14
November 2017

Generally, there are two control approaches for regulation of a PV array using boost converter; i.e. close loop and open loop controls. Reference [23] shows that in a PV array connected to the boost converter, the worst case from stability and dynamic response points of view, occurs when the array operates in constant current region and low irradiance level, where dynamic resistance of the array has its largest negative value.

This two-loop control method needs two PI controllers and an expensive current sensor. In contrast, in open loop control, which is a common method for boost converters control, there is no feedback, and the appropriate input voltage is generated considering the relation between the input voltage ( ) and output voltage ( ) of the converter as in (4).

$$v_{in} = v_{pv} = (1 - D)v_0 \qquad (3)$$

In this method, it is not necessary to measure the boost converter inductor current and an expensive current sensor is saved. However, the system response may have some steady state error and more transients than the close loop method. One of the important parameters in MPPT of a PV system is the sampling time. After applying a new command voltage to the converter, to prevent instability and disruption in MPPT, sampling from the array voltage and current must be done after settling the system transient response. Therefore, sampling time period must be more than this settling time.

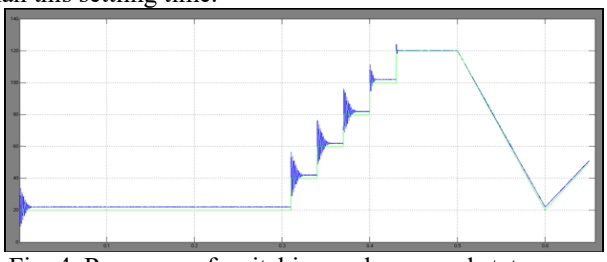

Fig. 4. Response of switching and averaged state space models of boost converter in PV system to step and ramp commands

For further analysis, response of a PV array connected to a boost converter with open loop control is studied through simulation in Matlab/Simulink environment. Converter parameters are presented in Table I and the simulated PV array has and . Output voltage of the boost converter is also considered constant at 250V.

Table I
Boost converter parameters

$r_L(\Omega)$	$L(uH)$	$C_{pv}(uF)$	Switching Frequency (kHZ)
0.3	600	100	20

Both the switching and averaged state space models of the system are simulated and their responses to step and ramp command signals by open loop control are shown in Fig. 4. Following conclusions are made from the system response:

1) Responses of the accurate switching model and the averaged state space model are almost identical.

2) The system response to step and ramp command signals contain some steady state error. This error can deteriorate the MPPT methods that are based on sampling from specific points of the array's P-V characteristic [13].

3) Oscillation, overshoot and settling time of the system to step commands is high, especially when the operating point in in the constant current region of the PV array, which impose higher switching stress and losses. In contrast, the ramp response has negligible transient.

4) Settling time of the system step response is about 15ms. Thus, for MPPT application, sampling time must be more than 15ms. It is noteworthy that is considered high, while in practice, for better efficiency, it is lower and results in higher settling time.

V PARTIAL SHADING CONDITION DETECTION

In this section, an algorithm for PSC detection is presented which is based on three criteria. Also, performance of the final algorithm is evaluated in various PS patterns.

PSI index as Partial Shading Condition Detection Criterion

The first proposed criterion is based on a new index that is defined as follows:

$$PSI = \frac{\Delta P}{\Delta V.P}\Big|V_{mpp-arr} = \frac{\frac{\partial P}{\partial V}}{V.I}\Big|V_{mpp-arr} = \frac{\frac{\partial (VI)}{\partial V}}{V.I}\Big|V_{mpp-arr} = 1Vmpp{-}arr{+}\partial II.\partial VVmpp{-}arr \qquad (4)$$

The criterion is normalized derivative of the PV array power respect to the array voltage at , which is similar to that used in IC method for MPPT. At UIC, PSI is zero. Under PSC, however, the local MPP voltage changes from , and therefore, PSI is not zero and is dependent on the shading pattern. According to Sec. II, when a PV string is under PSC, the voltage across the shaded module ( ) at is bound as follows:

$$\frac{N_s V_{mpp-mod} - n_{in} V_{oc-mod}}{N_s - n_{in}} < V_{mod-shaded} < V_{mpp-mod} \qquad (5)$$

From (6) two cases may arise for $\frac{\partial I}{I\partial V}\Big|V_{mpp-arr}$:

1) $N_s V_{mpp-mod} > n_{in} V_{oc-mod}$

In this condition, is positive and the absolute value of is less than its value in UIC, the local MPP of the string is in , and is positive

2) $N_s V_{mpp-mod} < n_{in} V_{oc-mod}$

In this case the shaded modules are bypassed with the bypass diodes, and . The insolated modules operate in the constant voltage region. Therefore, is much bigger than its value in UIC; PSI is negative and local MPP of the string is in .

International Journal of Research
Available at https://edupediapublications.org/journals
e-ISSN: 2348-6848
p-ISSN: 2348-795X
Volume 04 Issue14
November 2017

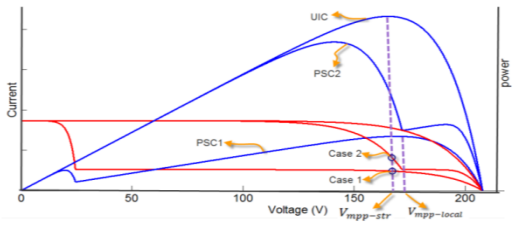

Fig. 5. I-V and P-V characteristics of PV string in different PSCs.

To investigate the effectiveness of the PSI index in PSC detection, behavior of a sample string, as a representative of an array, is analyzed in different PS patterns. For simplicity and without loss of generally, only two irradiance levels are considered in PSs.

According to the results of Sec. II and (3), it can be easily shown that in a shaded string, when is too high, the second local MPP ( ) will be near . Although the proposed algorithm may rarely mistake in detection of PSCs in the above-mentioned situations, but the main objective, which is GMPPT, is not lost. To prove this fact, a sample string under PSC (such as the PSCs in Fig. 5) is considered that has two local MPPs; the first one is in the range and has , and the next one is in with the following power relation:

$$P_{mpp\,-2} = V_{mpp\,-2} I_{mpp\,-2} \approx V_{mpp\,-2}\left(\frac{1}{IR}\right).I_{mpp\,-1} > (K+1)n_{in}V_{mpp\,-mod}\left(\frac{1}{IR}\right).I_{mpp\,-1} = (K+1)\left(\frac{1}{IR}\right)P_{mpp\,-1} \quad (6)$$

It is obvious that when IR is too low or K is too high (the same situation that PSI index may be near zero, e.g. PSC1 in Fig. 5), Therefore, if the PSI index mistakes in detection of this PSC, the conventional P&O algorithm used in the UICs tracks the second MPP which is the GMPPT.

Updating and Final PS Detection Criteria

Until now, it was supposed that is available for PSI evaluation. In practice, and are dependent on the type of modules and temperature as in (8); and also, there is some difference between the temperatures of the shaded and insolated modules.

$$V_{mpp\,-arr} = V_{mpp\,-arr\,-SC^*}\left(1-\rho_{arr}\,(T-25)\right) = \sum_{i=1}^{N_s} V_{mpp\,-mod\,-Sc^*} * \left(1-\rho_{mod\,-t}(T_t-25)\right) \quad (7)$$

where and are and in standard condition (S=), respectively. T is temperature and and are the temperature dependency coefficients of and , respectively. In the UIC, the operating voltage of the array is . Therefore, is available continuously. Also, its slight dependence on irradiance level can be updated easily, using the array current at . Under PSC, the operating voltage is not . Consequently, that is dominantly dependent on the temperature of the array is not available.

Accordingly, three cases may be fronted as follows:

1).The whole array is in UIC, and therefore, the temperature of all modules is the same as the sample module temperature. Thus, there is no error in updating in this case, and UIC can be detected using the PSI index.

2).The array is in PSC and the sample module is insolated. In this case because of the negative value of for all types of modules and in (8), the updated value of will be less than its real value. Therefore, the calculated value of PSI and the difference between the real local MPP voltage and the updated (named) will be greater than its real value. Hence, PS detection becomes easier.

3).The array is in PSC and the sample module is shaded. In this case, also because of the negative value of , the updated value of is greater than its real value. According to the above discussion, the PSI index criterion is reinforced with two other criteria. These two criteria are defined based on normalized values of and that are defined in the above. Finally, the criteria for PS detection will be as follows.

$$|PSI| > 0.001 \quad \left|\frac{\Delta V_{mpp\,-error}}{V_{mpp\,-error}}\right| > 0.02 \quad \left|\frac{\Delta V_{mpp\,-error}}{V_{mpp\,-error}}\right| > 0.02 \quad (8)$$

The specified thresholds in (9) are determined according to the simulations of many PS scenarios on various structures of PV array. Based on these criteria, the array is in the PSC if at least one of these conditions is met.

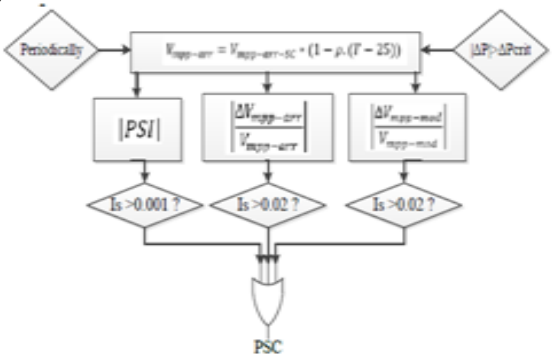

Fig. 6. Flow chart of the proposed algorithms for PS detection.

So far, the proposed algorithm is studied in a string of series modules. In (10), it is shown that PSI of an array is the weighted average PSI of individual strings, and therefore, using the PSI and two other criteria in (9) suffices for PS detection in any array.

$$PSI = \frac{\Delta P}{\Delta V.P}\left|V_{app\,-array} = \frac{\sum \Delta p_i}{\Delta V.\sum P_i}\right|V_{app\,-array} = \sum PSI_i \frac{P_i}{\sum P_i} \quad (9)$$

where and are the power of string and its differentiate, respectively

Effectiveness of proposed algorithm for PSC detection

International Journal of Research
Available at https://edupediapublications.org/journals
e-ISSN: 2348-6848
p-ISSN: 2348-795X
Volume 04 Issue14
November 2017

In the following, a sample array is simulated in different PSCs to verify the effectiveness of the proposed PS detection algorithm.

TABLE II.
Electrical data of module nd195r1s in standard test condition

P_{max}	V_{oc}	I_{sc}	V_{mpp}	I_{mpp}	P_{max} Termal Coefficeint	ρ_{mod}
195	29.7	8.68	23.6	8.27	-0.44 %/C·	-0.329%/C·

As shown in 0 , the array is 3x5, composed of ND195R1S modules with electrical data given in Table II.

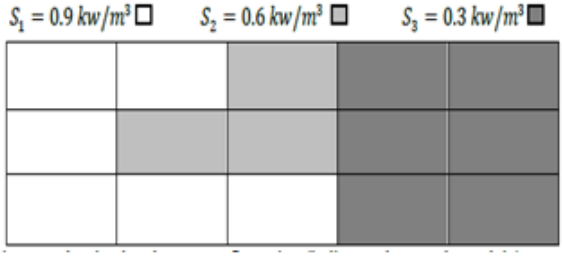

Fig. 7. The simulated array configuration (indicates the sample module).

As it was mentioned previously, robustness of the proposed method is reduced only under the PSCs that is too high and is too low, and it may be possible that the proposed method does not detect the PSC. In these situations, as proved in part B of this section, the local MPP, which is near , is the GMPP and the conventional P&O algorithm tracks it. Therefore, the final goal that is GMPPT is not missed.

Table III
Results of psc detection in sample pscs

	PSC1	PSC2	PSC3	PSC4	PSC5
PS Patterns	2-2-1	5-0-0	0-1-4	1-1-3	1-1-3
	1-3-1	3-1-1	0-0-5	1-1-3	5-0-0
	3-2-0	3-2-0	1-1-3	1-0-4	4-0-1
$\lvert PSI \rvert$	0.008	0.0036	0.002	0.003	4.00E-04
$\left\lvert \frac{\Delta V_{mpp-arr}}{V_{mpp-arr}} \right\rvert$	0.09	0.04	0.022	0.03	0.003
$\left\lvert \frac{\Delta V_{mpp-mod}}{V_{mpp-mod}} \right\rvert$	0.3	0	0.03	0.08	-0.08
PSC	yes	yes	yes	yes	yes

It is worth comparing the proposed PSC detection method with that of [11, 12]. Their method is based on observing a big power change, and is sensitive to the relevant threshold: a smaller threshold may cause wrong detection of PSC, and a bigger one may result in missing it. In contrast, the proposed method in this paper is activated in two ways: 1) periodically, 2) after observing a noticeable power change. For perfect detection of PS, the threshold of this power change can be set to lower values, because after observing the change, the criteria in (9) will be examined to rule out wrong PSC candidates. Also, in comparison to the method used in [18], which samples the array current in low and up voltages to detect PSC, the proposed method in this paper does not impose any big disturbance on the system as the method of [18] does.

VI PROPOSED ALGORITHM FOR MPPTUNDER PSC

MPPT is a time varying optimization problem, in which the objective function evaluation is done physically; i.e. by applying specific voltages to the array, its output power is measured after settling its voltage, whereas in the numerical optimization problems, function evaluation is done numerically and imposes calculation burden on the processor.

According to Sec. II, under PSC, the GMPP is in the following voltage region that must be searched for GMPPT:

$$V_{mpp-mod} < V < V_{oc-arr} \qquad (10)$$

A straight solution for GMPPT with minimum steps is that sampling from P-V characteristic of the array be done only in specific points [13]. In practice, these methods rely on approximations and cannot guarantee the GMPPT.

According to the above discussion, two important facts inspire using ramp voltage as the command signal of converter to search the voltage region of (11) for GMPPT:
1). In contrast to the response of the boost converter to step commands, settling time and transient of the boost converter to ramp command is nearly zero (Fig. 4).
To limit the search region for GMPPT, further analyses are presented as follows.

1) Assume a sample operating point of the array as . It is known that when the array voltage increases, its current decreases. Therefore, the array current ( ) for is lower than . Hence,

$$P_{arr}(V > V_S) = VI_{arr} < VI_s \qquad (11)$$

In addition, because the maximum voltage of the array is

$$P_{arr}(V > V_S) < V_{oc-arr} I_s \qquad (12)$$

Based on the above arguments, during positive ramp command, at any point in which is less than the last updated value for MPP ( ), the array power will also be less than at all upper voltages. Therefore, continuing the positive ramp command is not required. In other words, the search region will be limited to in which,

$$V_{oc-arr} I_s < P_e \qquad (13)$$

2) Whenever PS occurs after a UIC, negative ramp of MPPT process is bound as follows. For the voltages that the array power is less than and it is not needed to search this region. Hence, lower voltage of search region will be that

$$V_s < P_e / I_{sc} \qquad (14)$$

Besides, MPP current of PV arrays under UIC is about [3], and therefore is approximately known in term of .

The proposed MPPT method does not need any electrical characteristics of the PV array except to which is used to define the search region. All MPPT methods needs to know to know the search region. Flow chart of the proposed algorithm for MPPT in PSC is shown in Fig. 8.

International Journal of Research
Available at https://edupediapublications.org/journals
e-ISSN: 2348-6848
p-ISSN: 2348-795X
Volume 04 Issue14
November 2017

The ramp voltage can be implemented either with an analog rate limiter or digitally with small step changes in duty cycle.

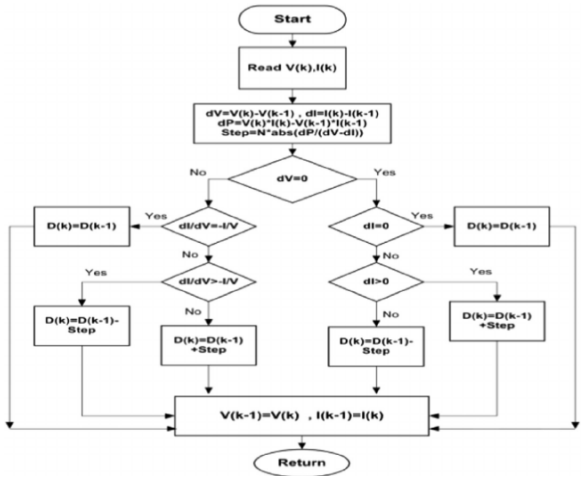

Fig. 8. Flow chart of the proposed algorithms for IC-MPP tracking under PSC.

For selection of the ramp rate, the following points are noted:

1)-Sampling rate of the array voltage and current must be coordinated with the ramp rate of command voltage.To achieve the GMPP voltage with maximum 1V error, at least one sample per each 2V interval is needed. Therefore, the minimum sampling rate must be

$$f_{sam} > \frac{4000}{200} * \frac{200}{2*1} = 2KHZ \qquad (15)$$

Since the existing micro-controllers have much faster sampling capability, no serious limitation on voltage ramp is imposed from this aspect.

INCREMENTAL CONDUCTANCE MPPT

In incremental conductance method the array terminal voltage is always adjusted according to the MPP voltage it is based on the incremental and instantaneous conductance of the PV module.

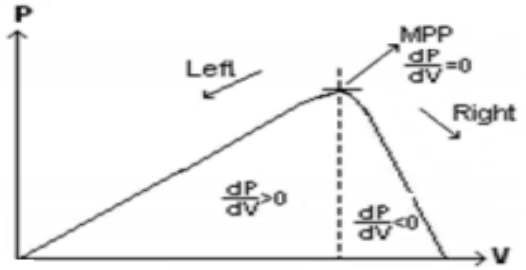

Fig-9: Basic idea of incremental conductance method on a P-V Curve of solar module

Fig-6 shows that the slope of the P-V array power curve is zero at The MPP, increasing on the left of the MPP and decreasing on the Right hand side of the MPP. The basic equations of this method are as follows.

$$\frac{dI}{dV} = -\frac{I}{V} \quad At\ MPP$$

$$\frac{dI}{dV} > -\frac{I}{V} \quad Left\ of\ MPP$$

$$\frac{dI}{dV} < -\frac{I}{V} \quad right\ of\ MPP \qquad (16)$$

When the ratio of change in output conductance is equal to the negative output conductance, the solar array will operate at the maximum power point.

INCRIMENTAL CONDUCTANCE MPPT ALGORITHM

This method exploits the assumption of the ratio of change in output conductance is equal to the negative output Conductance Instantaneous conductance. We have,

$$P = VI \qquad (17)$$

Applying the chain rule for the derivative of

$$\partial P/\partial V = [\partial(VI)]/\partial V$$

$$\partial P/\partial V = 0 \qquad (18)$$

The above equation could be written in terms of array voltage V and array current I as

$$\partial I/\partial V = -\ I/V \qquad (19)$$

The MPPT regulates the PWM control signal of the dc – to – dc boost converter until the condition: $(\partial I/\partial V) + (I/V) = 0$ is satisfied.

In this method the peak power of the module lies at above 98% of its incremental conductance. The Flow chart of incremental conductance MPPT is shown below.

VII SIMULATION RESULTS

In this section, performance of the proposed method for GMPPT in PSC is evaluated in various aspects using simulations and experiments.

Simulation Results

The proposed method is compared with the PSO-based algorithm with 3 primary particles presented. It is also compared with the method of [11], which is one of the best intelligent MPPT methods that is referenced very often.

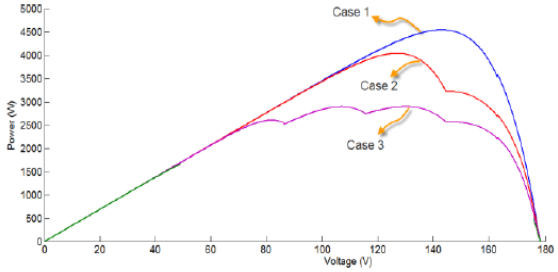

Fig. 10. P-V characteristics of array in UIC and two different PSCs.

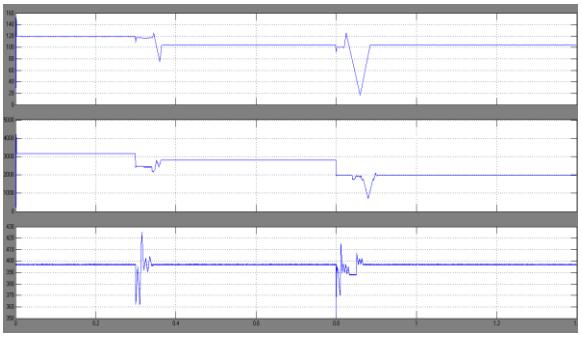

Fig. 11. MPPT process with the proposed and two other methods in different PSC patterns. 1.The proposed method: (a) array voltage, (c) array power, and (e) grid voltage.

Table IV
Comparison of three MPPT methods.

Criteria	The new proposed method	PSO base method in [19]	Proposed method in [11]
Speed of tracking	40ms (increasable)	About 500ms	More than 500ms
Transients and stress on converter	Low	High	Medium
Imposed transient voltages on the grid	Low	High	Medium
Energy loss	Low	High	High
Computational burden	Low	High	Medium
dependency to uniformity of modules	No	A little	Yes
Success probability	In all situations	Is not proved in all situations	almost in all situations

Since sampling from of the array P-V characteristic in these methods are done with specific intervals which depend on the model of modules, non-identical modules in the array affect their Efficiency.

CONCLUSION

According to the paper we are implementing a partial shading condition detection algorithm. There are placing a novel simple and fast algorithm which is denoted as the increment condition of MPPT under PSC that operates as direct control method and needs no feedback control of current and voltage. The IC algorithm was designed to control the duty cycle of Buck Boost converter and to ensure the MPPT work at its maximum efficiency. The wind energy system generates power in the form of AC with different voltage and frequency levels in case of variable speed operation. Wind power is cost-effective. According to the performance of the proposed GMPPT method we have following advantage which is given below:

1) It is simple and can be implemented with a cheap microcontroller like AVR;

2) It has a high adjustable speed;

3) Because of the smooth change of power in comparison with other methods, it has minimum negative impact on the connected power system; and 4) Its efficiency is guaranteed and is not dependent to the model of modules. Wind energy is a clean, renewable energy source and offers many advantages, which explains why it's one of the fastest-growing energy sources in the world. Research is aimed at improving technology, lowering costs, and addressing the challenges to greater use of wind energy.

REFERENCES

[1] T. Esram and P. L. Chapman, "Comparison of Photovoltaic Array Maximum Power Point Tracking Techniques," Energy Conversion, IEEE Transactions on, vol. 22, pp. 439-449, 2007

[2] Y.-J. Wang and P.-C. Hsu, "An investigation on partial shading of PV modules with different connection configurations of PV cells," Energy, vol. 36, pp. 3069-3078, 2011.

[3] D. Kun, B. XinGao, L. HaiHao, and P. Tao, "A MATLAB-Simulink-Based PV Module Model and Its Application Under Conditions of Nonuniform Irradiance," Energy Conversion, IEEE Transactions on, vol. 27, pp. 864-872, 2012.

[4] J. Young-Hyok, J. Doo-Yong, K. Jun-Gu, K. Jae-Hyung, L. Tae-Won, and W. Chung-Yuen, "A Real Maximum Power Point Tracking Method for Mismatching Compensation in PV Array Under Partially Shaded Conditions," Power Electronics, IEEE Transactions on, vol. 26, pp. 1001-1009, 2011.

[5] E. Koutroulis and F. Blaabjerg, "A New Technique for Tracking the Global Maximum Power Point of PV Arrays Operating Under Partial-Shading Conditions," Photovoltaics, IEEE Journal of, vol. 2, pp. 184-190, 2012.

[6] N. Tat Luat and L. Kay-Soon, "A Global Maximum Power Point Tracking Scheme Employing DIRECT Search Algorithm for Photovoltaic Systems," Industrial Electronics, IEEE Transactions on, vol. 57, pp. 3456-3467, 2010.

[7] Syafaruddin, E. Karatepe, and T. Hiyama, "Artificial neural network-polar coordinated fuzzy controller based maximum power point tracking control under partially shaded conditions," Renewable Power Generation, IET, vol. 3, pp. 239-253, 2009.

[8] I. Abdalla, J. Corda, and L. Zhang, "Multilevel DC-Link Inverter and Control Algorithm to Overcome the PV Partial Shading," Power Electronics, IEEE Transactions on, vol. 28, pp. 14-18, 2013.

[9] P. Sharma and V. Agarwal, "Exact Maximum Power Point Tracking of Grid-Connected Partially Shaded PV Source Using Current Compensation Concept," Power Electronics, IEEE Transactions on, vol. 29, pp. 4684-4692, 2014.

[10] C. Woei-Luen and T. Chung-Ting, "Optimal Balancing Control for Tracking Theoretical Global MPP of Series PV Modules Subject to Partial Shading," Industrial Electronics, IEEE Transactions on, vol. 62, pp. 4837-4848, 2015.